For our problem, we let $n \to 2n$ in the expression, Eq. (12), and we find that

$$\int \prod_{i=1}^{n} \frac{d^3p_i d^3q_i}{(2\pi)^6 4p_{i0}q_{i0}} (2\pi)^4 \delta^4\left(P - \sum_{i=1}^{n} p_i - \sum_{i=1}^{n} q_i\right) = \frac{1}{8\pi} \frac{2n-1}{[(2n-1)!]^2} \left(\frac{s}{16\pi^2}\right)^{2(n-1)} . \tag{13}$$

We find that the total cross section for the process $e^+e^- \to n\pi^+ n\pi^-$ is

$$\sigma(e^+e^- \to n\pi^+ n\pi^-) = \frac{8\alpha^4}{\pi(n!)^2} \left(\frac{m}{s}\right)^2 \frac{2n-1}{[(2n-1)!]^2} \left(\frac{3s}{16\pi^2 F_\pi{}^2}\right)^{2(n-1)} \left[\left(1 - \frac{m_\rho{}^2}{s}\right) \ln\left|1 - \frac{s}{m_\rho{}^2}\right| - \frac{1}{2}\left(1 - \frac{2m_\rho{}^2}{s}\right) \ln\left|1 - \frac{s}{2m_\rho{}^2}\right|\right]^2 . \tag{14}$$

Our expression, Eq. (14), for the total cross section is only partially valid because it is based on the soft-pion limit. Nevertheless, we may estimate magnitudes. If we chose the value $s = (6m_\pi)^2$ and $n = 2$, then it follows from Eq. (14) that $\sigma(e^+e^- \to 2\pi^+ 2\pi^-) \approx 10^{-44}$ cm^2. This is very small and thus we find that this two-photon-exchange diagram, Fig. 1, contributes negligibly. This is in contradiction to Brodsky, Kinoshita, and Terazawa[2] who, in their calculation, estimate the two-photon exchange to dominate over the one-photon exchange. Even if we consider the case that $s \sim 9$ GeV^2 and $n = 4$, it follows that the total cross section is $\sigma(e^+e^- \to 4\pi^+ 4\pi^-) \approx 10^{-47}$ cm^2. The one-photon exchange[1] is expected to dominate for e^+e^- → hadrons with no leptons in the final state where the total cross section varies as α^2.

We are grateful to Dr. William B. Kaufmann for discussions.

[1]J. D. Bjorken and S. J. Brodsky, Phys. Rev. D 1, 1416 (1970).

[2]N. Arteaga-Romero, A. Jaccarini, P. Kessler, and J. Parisi, Phys. Rev. D 3, 1569 (1971); S. J. Brodsky, T. Kinoshita, and H. Terazawa, Phys. Rev. Letters 25, 972 (1970).

[3]H. Terazawa, Phys. Rev. Letters 26, 1207 (1971).

[4]S. Weinberg, Phys. Rev. Letters 18, 507 (1967); T. Das, G. S. Guralnik, V. S. Mathur, F. E. Low, and J. E. Young, *ibid.* 18, 759 (1967).

[5]It may be noted that the form, Eq. (5), is obtained by symmetrization (Ref. 3) in the photons. Otherwise the denominator with σ^2 will appear with the square of the 4-momentum of one or the other photon.

[6]Reference 3, footnote 17; J. J. Sakurai, *Currents and Mesons* (University of Chicago Press, Chicago, 1969), p. 148.

PHYSICAL REVIEW D VOLUME 5, NUMBER 5 1 MARCH 1972

Electroproduction and the "Size" of a Virtual Photon

J. B. Kogut
Institute for Advanced Study, Princeton, New Jersey 08540
(Received 11 November 1971)

We consider the possibility that the radius of interaction between a virtual photon and a proton varies sensitively as the mass of the photon changes. This phenomenon is studied in quantum electrodynamics and in multiperipheral and constituent models. Physical arguments are also presented which claim that the radius of interaction should vary significantly as Q^2 changes from 0 to 1 GeV^2. If experiments confirm these expectations, then new and dramatic experimental tests of the presence of multiperipheral mechanisms in photon-initiated processes can be made.

I. INTRODUCTION

It has been conjectured by several authors that the angular distribution of ρ mesons produced in electroproduction reactions, $e + p \to e + \rho + p$, will spread as the magnitude of the invariant mass, $(Q^2)^{1/2}$, of the photon increases. If true, this prediction, originated by Cheng and Wu[1] and later rediscovered and discussed lucidly by Bjorken,[2,3] will allow us to test many of our present ideas concerning hadron reactions with improved sensitivity and new techniques. One investigation in this direction has been reported recently by Harari.[4] It is the purpose of this article to investigate the plau-

sibility of this conjecture (the "small photon" hypothesis) and to point out additional applications of the hypothesis.

We first discuss the small-photon prediction within the field-theoretic framework in which it was originally discovered. We compute off-shell Delbrück scattering using infinite-momentum techniques which expose the simple physical basis of the hypothesis. Furthermore, we numerically evaluate the effective impact parameter between the photon and the external field as a function of $(Q^2)^{1/2}$ and establish that the impact parameter changes significantly for experimentally accessible $(Q^2)^{1/2}$ (~0.5–1 GeV). This calculation suggests a more general physical argument which also claims, in the context of hadron physics, that the small-photon effect should be dramatic for small, accessible $(Q^2)^{1/2}$. We devote some time to these points since the proposed single-ρ and -π electroproduction experiments will be practical only for Q^2 less than ~1–2 GeV^2.

Next we suggest that variable-Q^2 electroproduction experiments will provide new and more sensitive tests of present ideas concerning strong-interaction dynamics. In particular, we deduce a striking implication of the multiperipheral model which should allow a *definitive test* of that model's relevance to these electroproduction processes.

We further test and elucidate our ideas by briefly considering a simple ladder model and finally a more elaborate model suggested by vector-meson dominance (VMD) and the constituent picture of deep-inelastic electron scattering. The simple ladder model, which has been studied by many authors in the past, predicts a considerably weaker Q^2 dependence of the $d\sigma/dt(ep \to epp)$ than the physical arguments abstracted from the QED (quantum electrodynamics) model. The second model, which may be more closely related to the real world, suggests the small-photon phenomena, but is not sufficiently restricted by known phenomenology or basic principles to allow a compelling calculation. However, the analysis of this model relates the physical ideas in the small-photon approach to conventional Regge approaches and may be of use phenomenologically when more data become available. In particular, the small-photon phenomena suggest that the Regge residue function at the virtual-photon–Pomeranchukon–ρ vertex should depend sensitively on the mass of the virtual photon.

The article closes with a short comment pointing out that the small-photon predictions apply only in that kinematic region where the scattering can proceed through a diffractive mechanism. The physical criterion leads to a familiar inequality involving the laboratory energy, ν, of the photon and its mass, $(Q^2)^{1/2}$ namely, $\nu \gtrsim 3 + 5Q^2$. This simple kinematic point has frequently been overlooked in the literature.

II. QUANTUM-ELECTRODYNAMIC MODEL

A. Off-Shell Delbrück Scattering

To begin, consider off-shell Delbrück scattering shown in Fig. 1. The incident electron beam produces an energetic photon of mass $(Q^2)^{1/2}$ which dissociates into a pair of charged constituents. Each member of the pair scatters via multiphoton exchange before forming a final outgoing state. An account of the calculation of the S matrix for this process is contained in Appendix A. The physics at work in this scattering process is most transparent when the scattering amplitude is written in configuration space. Using the notation of Appendix A, the S matrix becomes proportional to

$$M(\vec{q}' - \vec{q}, Q^2) = \int d\vec{R}\, e^{i(\vec{q}' - \vec{q})\cdot\vec{R}} M(\vec{R}, Q^2), \qquad (2.1)$$

where $M(\vec{R}, Q^2)$ is the configuration-space realization of the profile function for virtual-photon–external-field scattering; $\vec{q}' - \vec{q}$ is the momentum imparted to the photon by the external field; $\vec{R}$ is the position of the center of mass (infinite-momentum interpretation) of the pair measured from the origin of the external field. From Appendix A, the profile function reads

$$M(\vec{R}, Q^2) = \int d\vec{r}\, d\alpha \left(\exp\left\{ -i \left[\chi\left(\vec{R} + \frac{(1-\alpha)\vec{r}}{[\alpha(1-\alpha)Q^2 + \mu^2]^{1/2}} \right) - \chi\left(\vec{R} - \frac{\alpha\vec{r}}{[\alpha(1-\alpha)Q^2 + \mu^2]^{1/2}} \right) \right] \right\} - 1 \right) [(1-\alpha)^2 + \alpha^2] K_1^2(\vec{r}), \qquad (2.2)$$

where $\vec{r}$ is the relative distance (dimensionless) between members of the pair; α is the longitudinal fraction of one constituent relative to photon; μ is the constituent mass; χ is the eikonal phase; and $K_1(\vec{r})$ is a modified Bessel function of first order which is the configuration-space realization of the energy denominators and vertices controlling the size of the photon. The arguments of the eikonal phases are simply the positions of the members of the pair relative to the fixed external field.[2]

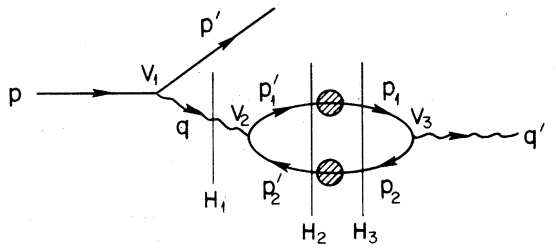

FIG. 1. Virtual-photon scattering off an external field. The shaded circles indicate multiple-photon exchange.

To understand Eqs. (2.1) we refer to Fig. 2 which projects the scattering event onto a transverse plane. The external field has a certain effective radius and the photon, by virtue of its constituents, also has a certain radius. Clearly, from Eq. (2.1) we see that the radius of the photon depends upon $(Q^2)^{1/2}$, μ, and α. There will be considerable scattering if the disks of Fig. 2 overlap. The maximum impact parameter is given by the transverse extension of the external field, R_T, plus the radius of the photon. As the invariant mass of the virtual photon increases, the transverse distance between the members of the pair decreases as implied by the uncertainty principle. So, the net impact parameter between the photon and the target decreases to the limit R_T as Q^2 increases, and the diffraction peak spreads accordingly.

It is of some interest to take this model and simply evaluate the net impact parameter as a function of Q^2. To do this we average R^2 over the profile function,

$$\langle R^2(Q^2)\rangle \equiv \frac{\int R^2 M(\vec{R}, Q^2)d\vec{R}}{\int M(\vec{R}, Q^2)d\vec{R}}. \tag{2.3}$$

In the QED model we choose the external field to be a screened Coulomb field. The eikonal appearing in Eq. (2.3) becomes

$$\chi(\vec{x}) = e\int_{-\infty}^{\infty} \frac{\exp[-\mu(\vec{x}^2+z^2)^{1/2}]}{(\vec{x}^2+z^2)^{1/2}}dz$$
$$= 2eK_0(\mu|\vec{x}|). \tag{2.4}$$

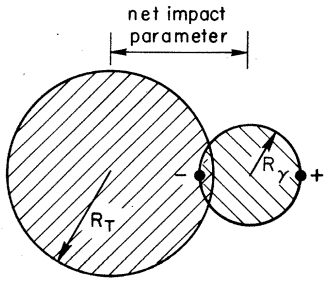

FIG. 2. A visualization in the transverse plane of off-shell Delbrück scattering.

Here we have chosen the inverse screening length to be μ, which means that we are supposing the on-shell photon to have approximately the same spatial extent as the external field. The motivation for this assumption comes from hadron physics in which ρ mesons, protons, etc. all have about the same size. Now Eq. (2.3) can be evaluated numerically and the resulting curve is shown in Fig. 3. To interpret the curve quantitatively we must specify the mass μ. The most reasonable range of choices would seem to lie between one and two pion masses. This choice then gives the external field (proton) a spatial radius of between 1.4 and 0.7 F. From Fig. 3 we also see that $R^2(Q^2)$ has fallen to half its $Q^2=0$ value by Q^2 in the neighborhood of 1 GeV^2. So, and this is the point of doing the numerical exercise, in this simple model the photon's radius *changes significantly* for experimentally accessible Q^2.

This model calculation is intended simply to illustrate a kinematic mechanism which may be present in the real world. Of course, the details of the dynamics of the QED calculation are probably irrelevant. Recognizing that fact we now attempt to merge the reasonable aspects of the QED calculation with some basic facts about real hadrons into another argument for the small-photon hypothesis.

B. A Geometric Argument

Discard the details of the QED model momentarily and consider actual photon scattering off a target proton. We must ask what dimensional quantities in the scattering process control the shape of the diffraction peak. Apparently, they are the intrinsic sizes of the hadronic component

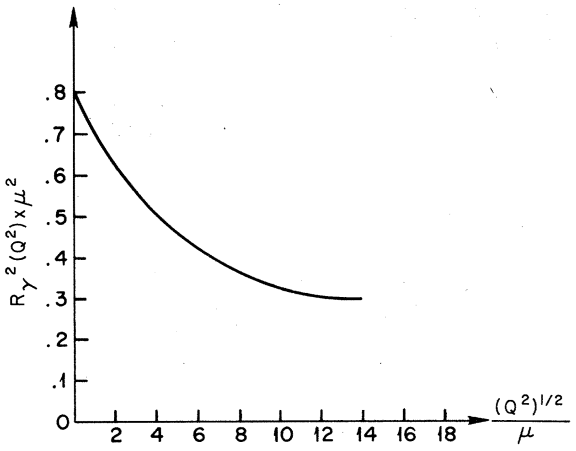

FIG. 3. The mean squared interaction radius for virtual-photon–external-field scattering plotted as a function of the mass, $(Q^2)^{1/2}$, of the photon.

of the on-shell photon and the target proton. But these sizes are on the order of 1 F $\approx$ (200 MeV)$^{-1}$. Now allow the photon to become virtual. Once $(Q^2)^{1/2}$ becomes 0.5–1 GeV it dwarfs the other dimensions in the problem and it alone should characterize the size of the photon, i.e., once $(Q^2)^{1/2} \sim 0.5$–1 GeV, the spatial extent of the photon, $R_\gamma(Q^2)$, should be just that given by dimensional analysis, $1/(Q^2)^{1/2}$.[5] Of course, there are other large masses in the problem, such as the mass of the proton. However, the spatial extent of the proton is characterized by several pion masses and the geometric approach claims that only this dimension controls the slope of the diffraction peak. In particular, if the hadronic component of the on-shell photon has a transverse size comparable to that of the target, one would predict that the t distribution of diffractively produced ρ's would spread by a factor of about 4 as Q^2 increases to, say, 1–2 GeV^2. This follows since the diffractive picture advocated here suggests that the t dependence of the elastic virtual γ + proton $\to \rho$ + proton cross section reads approximately

$$\frac{d\sigma}{dt} \sim \exp[-\tfrac{1}{2}\langle R^2(Q^2)\rangle t], \tag{2.5}$$

where $\langle R^2(Q^2)\rangle$ is the mean squared impact parameter which initiated the process.

III. HADRONIC MODELS

A. Multiperipheral Dynamics

We wish to investigate whether the ideas discussed in Sec. II survive a more realistic treatment of strong-interaction dynamics. In this pursuit we immediately face the impasse that there are no known basic principles to guide us in this direction. The electroproduction experiments of interest represent new ground for theoretical speculations. It therefore seems somewhat premature to delve too deeply into detailed strong-interaction models. Rather, we are content to expose a few general features of various models which will prove easily observable in the first round of experiments. Elaboration and sharpening (or rejection) of our observations should certainly wait until experiments indicate whether the small-photon conjecture is on the right track or not.

We consider multiperipheral models in general. Interestingly, it will not be difficult to test the proposition that multiperipheral dynamics are playing a role in electroproduction. Consider Fig. 4 which depicts a very inelastic process occurring through a multiperipheral mechanism. As usual, one imagines that the fastest secondaries emerge from the top of the chain, the fragmentation region of the photon. These secondaries feel the effect of the Q^2 of the photon most strongly, and, as in the QED model, their average transverse momentum will grow with Q^2. Inspection of the energy denominators implicit in Fig. 4 confirms this point. However, multiperipheral chains are characterized by short-range order, which in this case implies that the secondaries emerging from further down the chain do not feel the effect of the mass of the photon so keenly. This implies that the average transverse momentum of the slow secondaries should be small and insensitive to Q^2. So, a plot of the secondaries in a particular event should appear as shown in Fig. 5. The *absence* of such a curious correlation of $p_\parallel$ and p_T and its characteristic dependence on Q^2 would shed considerable doubt on the relevance of multiperipheral mechanisms to photoproduction and electroproduction. In fact, the more general concept of short-range order in rapidity will receive a *severe* test by this proposal.[6]

Of course there will be some fairly high-multiplicity events arising from diffraction dissociation. These will not necessarily exhibit the correlation effect explained here. However, Wilson[6] has argued that this mechanism should not populate the central region in the rapidity between the photon and the target and this is known experimentally to be the case in electroproduction for $\nu \geq 10$ GeV. So, by selecting secondaries (pions, say) here and plotting their $\langle p_T\rangle$ parametrized by Q^2, one should be able to effectively eliminate the diffraction-dissociation events and search for the interesting correlations suggested here.

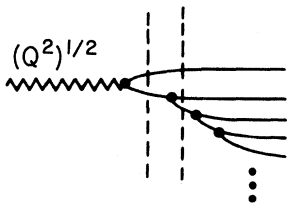

FIG. 4. A multiperipheral chain in a photon-initiated process.

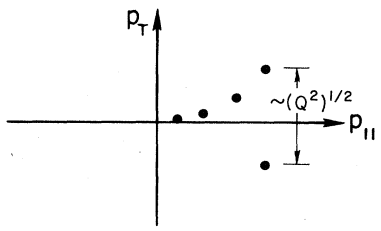

FIG. 5. The longitudinal-transverse momentum distribution of the secondaries in Fig. 4.

B. Basic Ladder Model

Consider the diagrams shown in Fig. 6. The particles composing the ladder are assumed for simplicity to be scalars which interact through the familiar $\lambda\phi^3$ coupling. We are interested in such processes as the external photons become virtual. To begin, ignore the spin of the photon. The scattering amplitude with spin properly accounted for will be considered briefly later. With this simplification the problem reduces to one often studied in the literature.[7] We remind the reader that the scattering amplitude assumes the expected Regge form

$$M(s, t) \sim \beta(t, Q^2, Q^2) s^{\alpha(t)} \beta(t, M_T^2, M_T^2), \qquad (3.1)$$

where β is the residue function and we have explicitly displayed its dependence on the squared momentum transfer t and the invariant masses of the external legs. Writing a Bethe-Salpeter equation to sum the ladder diagrams results in an integral equation which, in principle, determines the trajectory function $\alpha(t)$ and the residue function up to an over-all function of t. Unfortunately, these equations have been solved only in rather unrealistic models. For example, if one approximates the $\lambda\phi^3$ ladder model integral equation with a separable kernel, one can solve for the residue function and find that[8]

$$\beta(t, Q^2, Q^2) \sim (m_0^2 + Q^2 + \tfrac{1}{4}t)^{-\alpha(t)-1}, \qquad (3.2)$$

where m_0 is the mass of the horizontal rungs in the ladder. Although this equation exhibits the small-photon phenomenon, it only does so *weakly* as compared to the simpler geometric models [cf. Eq. (2.5)]. It will be interesting to see whether Eq. (3.2) or Eq. (2.5) is favored experimentally.

The reason for the relatively weak Q^2 behavior of Eq. (3.2) lies in the fact that the ladder model does not treat the photon end of the ladder preferentially. Our geometric arguments were based on the notion that one could separately consider first the development of the incident photon into a set of constituents, and second, the interaction of these constituents with the target. Such a distinction is not possible even in principle within this ladder model. It is also clear that if we included the spin of the photon properly, Eq. (3.2) would not have changed dramatically.[9] In Sec. III C we will consider a model which merges the more reasonable features of the geometric model with the ladder model.

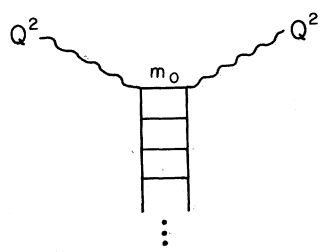

FIG. 6. Simple scalar ladder model.

C. Extended Ladder Model

In constructing a more sensible picture of photon processes for small $(Q^2)^{1/2}$ and large ν we turn to vector-meson dominance. In this approach one supposes that the virtual photon transforms into an off-shell vector meson which subsequently scatters off the proton. As ν grows the lifetime of the virtual ρ state increases proportionally, while the time duration of the interaction between the ρ and the proton presumably remains finite. From the point of view of constituent models, this fact suggests Fig. 7 as a first attempt to merge these two physical pictures. Clearly vector dominance alone cannot make a prediction concerning the spread of the ρ peak with Q^2. One must have some notion of the distribution of the hadronic matter in the ρ in order to proceed. But this is just what the constituent models purport to provide.

Unfortunately, we cannot actually calculate a scattering amplitude from Fig. 7 without knowing the amplitude that a photon consists of, say, two strongly interacting constituents. Model calculations can be attempted (s-channel ladder graphs, perhaps), but we refrain from that here. Instead we will just discuss the general form of the scattering amplitude in order to relate the small-photon hypothesis to more conventional approaches to this subject.

The details of the calculation of off-shell Delbrück scattering according to Fig. 7 can be found in Appendix B where additional motivation for this approach is also discussed. Clearly the amplitude consists of two parts: a wave function, V, which describes the composition of the photon as a pair of constituents, and the interaction of a constituent with the target through a multiperipheral mechanism. From Appendix B, Eq. (B6) we have the

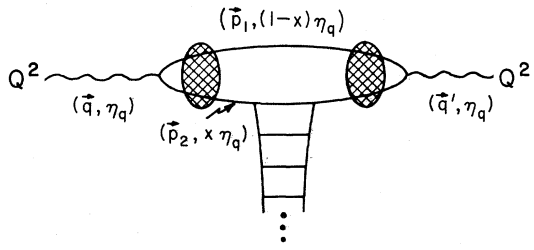

FIG. 7. A ladder model suggested by vector-meson dominance and the constituent picture of hadrons.

scattering amplitude

$$S(\vec{q}'-\vec{q}) \sim (\text{residue function for target}) s^{\alpha(t)} (\text{effective residue function for photon}), \tag{3.3}$$

where $t=-(\vec{q}'-\vec{q})^2$ and the residue function for the photon reads

$$\beta_\gamma(t, Q^2)=\int d\vec{p}dx \frac{V(Q^2, \vec{q}; \vec{p}, x)}{x(1-x)Q^2+\vec{p}^2+\mu^2}\beta\left(t, -\frac{\vec{p}^2+x\mu^2+x(1-x)Q^2}{1-x}, -\frac{\vec{p}'^2+x\mu^2+x(1-x)Q^2}{1-x}\right) x^{\alpha(t)} \frac{V(Q^2, \vec{q}'; \vec{p}', x)}{x(1-x)Q^2+\vec{p}'^2+\mu^2}, \tag{3.4}$$

where $\vec{p}$ is the relative momentum of a pair of constituents before scattering; $\vec{p}'=\vec{p}-(1-x)(\vec{q}'-\vec{q})$ is the relative momentum of the pair after scattering; and $V(Q^2, \vec{q}; \vec{p}, x)$ is the wave function of the photon. In order to calculate $\beta_\gamma(t, Q^2)$ one needs a realistic model for V which is quite beyond our reach. However, we can qualitatively understand how the t distribution is effected by changing Q^2 by inspecting Eq. (3.4). As Q^2 increases, larger values of $\vec{p}$ contribute significantly to the integral. This follows from the character of the energy denominators (Sec. II), the residue function β (Sec. III B), and the wave function V itself.[10] But this means, as shown in the QED model, that the photon is becoming smaller in configuration space which means the angular distribution of the secondaries should expand. Of course, the rate of angular spread with increasing Q^2 depends upon the actual dynamics controlling the wave function.

It is clear that in this approach the interesting physics is contained in three transverse distances as indicated in Fig. 8. First there is the photon size $R_\gamma(Q^2)$, then the size of the interaction region, $R_{\text{int}}(Q^2, s)$, and the size of the target, R_T. Several limiting kinematic cases are interesting. First, if the interaction is generated by multiperipheral mechanisms, $R_{\text{int}}(Q^2, s) \sim (\ln s)^{1/2}$. For $\ln s \gg 1$, this dimension will dwarf all others in the problem and the angular distribution of secondaries becomes independent of Q^2. Clearly, in this limit the intrinsic sizes of the photon and target become negligible and the physical picture approaches that of the simple ladder model discussed in Sec. III B. However, for presently accessible s, $\ln s$ is not large, and we expect $R_\gamma(Q^2)$ and R_T to be comparable. Then the physical picture resembles the QED model of Sec. II, and we would expect the small-photon predictions to apply. Unfortunately we cannot predict the function $R_\gamma(Q^2)$: We can only suggest a physically appealing way of interpreting the anticipated experimental results. However, on the basis of the QED model, the geometric argument, and the ideas in Eq. (3.4), we expect the small-photon predictions to apply to the upcoming electroproduction experiments.

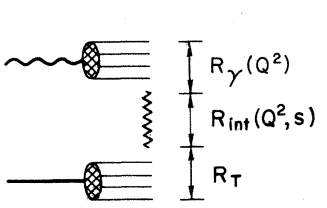

FIG. 8. The important transverse distances controlling the physics of Fig. 7.

D. A Comment on Kinematics

Our final remark concerns the region in the Q^2 and ν plane where we expect the small-photon prediction to apply. As argued at length, our physical picture applies only if the virtual photon of mass $(Q^2)^{1/2}$ and laboratory energy ν develops hadronic constituents before interacting with the target proton. Furthermore, this virtual state must be so long-lived that we can neglect its time development while it is within the range of interaction of the target. These criteria are presumably the ones which define the kinematic region in which electroproduction proceeds diffractively. To estimate the lifetime of the virtual hadron state one simply computes the reciprocal of the energy difference, ΔE, of that state and the incident photon. Of course, for a given ν the lifetime shortens as the photon becomes more virtual. Next one requires that the lifetime be greater than the diameter of the proton. This argument, which is familiar from discussions of VMD and has been made in the context of electroproduction before, leads straightforwardly to the inequality[11]

$$\nu \geq 3+5Q^2, \tag{3.5}$$

where all quantities are measured in GeV units. Unfortunately, the argument is not precise enough to indicate whether the inequality sign can be interpreted strictly, or if it should be replaced by "$\gg$." However, it is certain that the small-photon idea cannot be expected to apply if Eq. (3.6) is strongly violated.

Preliminary results from both SLAC and Cornell

have recently been reported. Neither experiment is conclusive. However, the indications, especially from the higher-energy SLAC experiment, are encouraging. Unfortunately some of the data recently reported do not satisfy inequality (3.6) above and, hence, do not represent a clear test of the small-photon hypothesis.

Note added in proof. Professor D. Yennie has pointed out to us that for many scattering processes it is the *squares* of the radii of the projectile and target which add. For such models the $\langle R^2(Q^2)\rangle$ appearing in Eq. (2.5) becomes $R_\gamma{}^2(Q^2)+R_T{}^2$, which suggests that the t distribution of diffractively produced ρ's should spread by a factor of 2 instead of the factor 4 appearing in the text. Unfortunately, the model of Sec. II A is not a reliable guide to this problem because of the singular character of the screened Coulomb potential.

ACKNOWLEDGMENTS

This work was suggested and aided by conversations with J. D. Bjorken. Discussions with H. Harari, L. Susskind, T. M. Yan, and H. D. I. Abarbanel are gratefully acknowledged. The author also thanks G. Farrar and A. Zee for reading the manuscript. The author is grateful to Dr. Carl Kaysen for his hospitality at the Institute for Advanced Study.

APPENDIX A

In this Appendix we will discuss the QED model calculation in some detail. We consider Fig. 1 and write the scattering amplitude according to the rules of infinite-momentum perturbation theory,

$$S_{fi}=\frac{e^3}{(2\pi)^4}(2\eta 2\eta')^{1/2}\delta(\eta-\eta'-\eta_q)\int d\vec{p}_1 d\vec{p}_1'\,\frac{d\eta_1}{2\eta_q}\,\frac{V_1V_2V_3}{(H_i-H_1)(H_i-H_2)(H_f-H_3)}$$
$$\times[F(\vec{p}_1-\vec{p}_1')F_c(\vec{p}_2-\vec{p}_2')-(2\pi)^4\delta(\vec{p}_1-\vec{p}_1')\delta(\vec{p}_2-\vec{p}_2')], \tag{A1}$$

where V_i and H_i denote the vertices and energy denominators, respectively, as indicated in the figure. As usual it is best to introduce kinematic variables which are suggested by the structure of the Poincaré group at infinite momentum. We define the relative momentum (two-dimensional) of the pair before the interaction as

$$\frac{\vec{k}}{\eta_r}=\frac{\vec{p}_1'}{\eta_1}-\frac{\vec{p}_2'}{\eta_2},\quad \frac{1}{\eta_r}=\frac{1}{\eta_1}+\frac{1}{\eta_2} \tag{A2}$$

and the relative momentum after the interaction,

$$\frac{\vec{k}'}{\eta_r}=\frac{\vec{p}_1}{\eta_1}-\frac{\vec{p}_2}{\eta_2}. \tag{A3}$$

Then the energy denominators can be written compactly,

$$\begin{aligned}
H_i-H_1&=\frac{\vec{p}^2+\mu^2}{2\eta}-\frac{\vec{q}^2}{2\eta_q}-\frac{\vec{p}'^2+\mu^2}{2\eta'}=-\frac{Q^2}{2\eta_q},\\
H_i-H_2&=\frac{\vec{p}^2+\mu^2}{2\eta}-\frac{\vec{p}'^2+\mu^2}{2\eta'}-\frac{\vec{p}_1'^2+\mu^2}{2\eta_1}-\frac{\vec{p}_2'^2+\mu^2}{2\eta_2},\\
H_i-H_2&=-\frac{Q^2}{2\eta_q}-\frac{\eta_q}{2\eta_1\eta_2}(\vec{k}^2+\mu^2),\\
H_f-H_3&=-\frac{Q^2}{2\eta_q}-\frac{\eta_q}{2\eta_1\eta_2}(\vec{k}'^2+\mu^2).
\end{aligned} \tag{A4}$$

Next, the vertices are simple and have been tabulated elsewhere.[2] Choosing the photons to have positive helicity and summing over the possibilities of e^+-e^- helicities, one obtains

$$\sum_{e^+,e^-\ \text{spins}} V_1V_2V_3=q_-\left(\frac{\eta}{\eta_1}\right)\frac{\eta_q}{\eta_1{}^2\eta_2{}^2}\left[\left(\frac{\eta_2}{\eta_q}\right)^2+\left(\frac{\eta_1}{\eta_q}\right)^2\right]k_+k'_-, \tag{A5}$$

where we have neglected the electron mass, and $k_\pm=(1/\sqrt{2})(k_x\pm ik_y)$. Furthermore, if we define the dimensionless variable

$$\alpha=\frac{\eta_1}{\eta_q},\quad 0\leq\alpha\leq 1 \tag{A6}$$

and eliminate the arguments of the eikonal factors in Eq. (A1) in favor of relative momenta and α,

$$\vec{p}_1-\vec{p}_1'=\vec{k}'-\vec{k}+\alpha(\vec{q}'-\vec{q}),\quad \vec{p}_2-\vec{p}_2'=\vec{k}-\vec{k}'+(1-\alpha)(\vec{q}'-\vec{q}), \tag{A7}$$

we have a more convenient expression for the scattering amplitude,

$$S(\vec{q}'-\vec{q})=-\frac{4e^3}{(2\pi)^4}\frac{\eta}{\eta'}\frac{q_-}{Q^2}(2\eta 2\eta')^{1/2}\delta(\eta-\eta'-\eta_q)$$
$$\times\int d\vec{k}d\vec{k}'d\alpha\,\frac{[(1-\alpha)^2+\alpha^2]k_+k_-'}{[\alpha(1-\alpha)Q^2+\vec{k}^2+\mu^2][\alpha(1-\alpha)Q^2+\vec{k}'^2+\mu^2]}$$
$$\times[F(\vec{k}'-\vec{k}+\alpha(\vec{q}'-\vec{q}))F_c(\vec{k}-\vec{k}'+(1-\alpha)(\vec{q}'-\vec{q}))-(2\pi)^4\delta(\vec{k}'-\vec{k}+\alpha(\vec{q}'-\vec{q}))\delta(\vec{k}-\vec{k}'+(1-\alpha)(\vec{q}'-\vec{q}))]. \tag{A8}$$

As discussed in the text, it is better to write S in configuration space. Introduce the infinite-momentum "center-of-mass" coordinates for the pair,

$$\vec{r}=\vec{x}_1-\vec{x}_2,\quad \vec{R}=\alpha\vec{x}_1+(1-\alpha)\vec{x}_2, \tag{A9}$$

and recall that

$$F(\vec{p})=\int d\vec{x}\,e^{-i\vec{p}\cdot\vec{x}}e^{-i\chi(\vec{x})}. \tag{A10}$$

The S-matrix element may now be written,

$$S(\vec{q}'-\vec{q})=-\frac{2e^3}{(2\pi)^4}\frac{\eta}{\eta'}\frac{q_-}{Q^2}(2\eta 2\eta')^{1/2}\delta(\eta-\eta'-\eta_q)M(\vec{q}'-\vec{q}), \tag{A11}$$

where

$$M(\vec{q}'-\vec{q})=\int d\vec{R}\,e^{-i(\vec{q}'-\vec{q})\cdot\vec{R}}\int d\vec{r}d\alpha(\exp\{-i[\chi(\vec{R}+(1-\alpha)\vec{r})-\chi(\vec{R}-\alpha\vec{r})]\}-1)$$
$$\times\{[(1-\alpha)^2+\alpha^2][\alpha(1-\alpha)Q^2+\mu^2]K_1^2([\alpha(1-\alpha)Q^2+\mu^2]^{1/2}|\vec{r}|)\}. \tag{A12}$$

Finally, we write $M(\vec{q}'-\vec{q})$ in terms of the dimensionless variable

$$\vec{\xi}=[\alpha(1-\alpha)Q^2+\mu^2]^{1/2}\vec{r}. \tag{A13}$$

Then,

$$M(\vec{q}'-\vec{q})=\int d\vec{R}\,e^{-i(\vec{q}'-\vec{q})\cdot\vec{R}}\int d\vec{\xi}d\alpha[(1-\alpha)^2+\alpha^2]K_1^2(\xi)$$
$$\times\left(\exp\left\{-i\left[\chi\left(\vec{R}+\frac{(1-\alpha)\vec{\xi}}{[\alpha(1-\alpha)Q^2+\mu^2]^{1/2}}\right)-\chi\left(\vec{R}-\frac{\alpha\vec{\xi}}{[\alpha(1-\alpha)Q^2+\mu^2]^{1/2}}\right)\right]\right\}-1\right). \tag{A14}$$

This form for the scattering amplitude is very transparent since one can read the profile function off without further manipulation. One can also examine Eq. (A14) for the dimensional argument presented in Sec. II B.

APPENDIX B

We will calculate here the scattering amplitude for Fig. 7. First there is the photon wave function which expresses the amplitude that the photon dissociate into a pair of fast partons: $V(Q^2, \vec{q}; \vec{p}, x)$. As usual we find it convenient to parametrize the kinematics of the pair by their relative momentum $\vec{p}$ and the longitudinal fraction x as in the QED model. The parton with longitudinal fraction x interacts with the target through Pomeranchukon exchange which is generated by the wee partons in the wave function of the photon.[12] We presume that we can characterize the Pomeranchukon exchange by multiperipheral mechanisms and write

$$\beta(t, M_1^2, M_2^2)(xs)^{\alpha(t)} \tag{B1}$$

for this subscattering. Here M_1 (M_2) is the invariant mass of the parton of fraction x before (after) the Pomeranchukon exchange. The invariant masses can be evaluated,

$$M_1^2 = 2x\eta_q\left(\frac{\vec{q}^2 - Q^2}{2\eta_q} - \frac{\vec{p}_1^{\,2} + \mu^2}{2(1-x)\eta_q}\right) - \vec{p}_2^{\,2},$$
$$M_1^2 = -\frac{1}{(1-x)}[\vec{p}^2 + x(1-x)Q^2 + x\mu^2], \tag{B2}$$

and, similarly,

$$M_2^2 = -\frac{1}{(1-x)}[\vec{p}'^2 + x(1-x)Q^2 + x\mu^2], \tag{B3}$$

where $\vec{p}'$ is the relative momentum of the pair after the scattering,

$$\vec{p}' = \vec{p} - (1-x)(\vec{q}' - \vec{q}). \tag{B4}$$

Finally, the energy denominators and further kinematics can be borrowed from Appendix A. The result becomes

$$M(\vec{q}' - \vec{q}) = \int d\vec{p}dx\, \frac{V(Q^2, \vec{q}; \vec{p}, x)}{x(1-x)Q^2 + \vec{p}^2 + \mu^2}\beta(t, M_1^2, M_2^2)\frac{V(Q^2, \vec{q}'; \vec{p}', x)}{x(1-x)Q^2 + \vec{p}'^2 + \mu^2}(xs)^{\alpha(t)}\beta(t, M_T^2, M_T^2), \tag{B5}$$

where M_1 and M_2 are given above, $t = -(\vec{q}' - \vec{q})^2$, and $\beta(t, M_T^2, M_T^2)$ is the residue function for the target. In the text we wrote Eq. (B5) in the more suggestive form,

$$M(\vec{q}' - \vec{q}) = \beta(t, M_T^2, M_T^2)s^{\alpha(t)}\left(\int d\vec{p}dx\, \frac{V(Q^2, \vec{q}; \vec{p}, x)}{x(1-x)Q^2 + \vec{p}^2 + \mu^2}\beta(t, M_1^2, M_2^2)\frac{V(Q^2, \vec{q}'; \vec{p}', x)}{x(1-x)Q^2 + \vec{p}'^2 + \mu^2}x^{\alpha(t)}\right) \tag{B6}$$

in order to express the fact that the dynamics of interest lie in the residue function for the photon.

---

[1]H. Cheng and T. T. Wu, Phys. Rev. Letters 22, 1409 (1969).

[2]J. D. Bjorken, J. B. Kogut, and D. E. Soper, Phys. Rev. D 3, 1382 (1971).

[3]J. D. Bjorken, SLAC Report No. SLAC-PUB-905, in the Proceedings of the Conference on Duality and Symmetry in Hadron Physics, Tel-Aviv, 1971 (unpublished).

[4]H. Harari, Phys. Rev. Letters 27, 1028 (1971).

[5]Actually in the QED model the inevitable logarithms appear. However, their variation in Q^2 is slow compared to $1/(Q^2)^{1/2}$.

[6]For additional tests of this hypothesis see K. Wilson, Cornell Report No. CLNS-131, 1970 (unpublished).

[7]H. D. I. Abarbanel, M. L. Goldberger, and S. B. Treiman, Phys. Rev. Letters 22, 500 (1969); H. Cheng and T. T. Wu, DESY report (unpublished).

[8]H. D. I. Abarbanel (private communication).

[9]In fact, including spin will slightly weaken the Q^2 dependence of the residue function.

[10]For example, an s-channel ladder model for V possesses this property.

[11]H. T. Nieh, Phys. Rev. D 1, 3161 (1970).

[12]R. P. Feynman, Phys. Rev. Letters 23, 1415 (1969).